34th Annual International Conference of the IEEE EMBS
San Diego, California USA, 28 August - 1 September, 2012

Simulation based efficiency prediction of a Brushless DC drive applied in Ventricular Assist Devices

André Pohlmann and Kay Hameyer

***Abstract*— Ventricular Assist Devices (VADs) are mechanical blood pumps that support the human heart in order to maintain a sufficient perfusion of the human body and its organs. During VAD operation blood damage caused by hemolysis, thrombogenecity and denaturation has to be avoided. One key parameter causing the blood's denaturation is its temperature which must not exceed 42 °C. As a temperature rise can be directly linked to the losses occuring in the drive system, this paper introduces an efficiency prediction chain for Brushless DC (BLDC) drives which are applied in various VAD systems. The presented chain is applied to various core materials and operation ranges, providing a general overview on the loss dependencies.**

I. INTRODUCTION

According to the World Health Organization [1], the major causes of death in industrialized countries are related to cardio vascular diseases. If a pharmaceutical based therapy for a patient suffering from terminal heart disease fails, the last clinical option is a donor heart transplantation. Although the demand for donor organs is rising worldwide, the number of transplantations has nearly been constant during the last years [2]. Due to the demand of alternatives, the field of Artificial Hearts has become a prominent research topic. In general Artificial Hearts can be categorized as Total Artificial Hearts (TAH) replacing the human heart and Ventricular Assist Devices (VADs) supporting the human heart. Furthermore VADs are divided into left-, right or biVADs according to the supported ventricle(s). Currently a TAH can only bridge the time until a donor organ is available. If the human heart remains some perfusion capabilities, a VAD can support it and in some cases the heart might recover due to the reduced load in the ventricle(s). A brushless direct current motor (BLDC) with permanent magnet excitation offers the advantage of a flat and energy efficient design. In combination with a noncontact bearing and a sensorless control it offers a high reliability and low maintenance effort. These advantages are beneficial for an artificial organ implantation providing a long-term assist. For this reason the BiVAD BiVacor [3], the VADs DuraHeart^{TM} [4] and Worldheart [5] and further VAD systems are actuated with a BLDC drive system. Essential requirements for a VAD are ensuring a sufficient perfusion of the human body while keeping damage to the blood and cell structure caused by the discussed reasons to a minimum. When seperating a VAD into its pump and drive system, the requirement of a sufficient perfusion and denaturation avoidance by overheating can directly be linked to the efficiency of the drive system, because its losses are dissipated into heat.

A. Pohlmann is with the Institute of Electrical Machines, Faculty of Electrical Engineering, RWTH Aachen University, Aachen, Germany andre.pohlmann at iem.rwth-aachen.de

K. Hameyer is with the Institute of Electrical Machines, Faculty of Electrical Engineering, RWTH Aachen University, Aachen, Germany kay.hameyer at iem.rwth-aachen.de

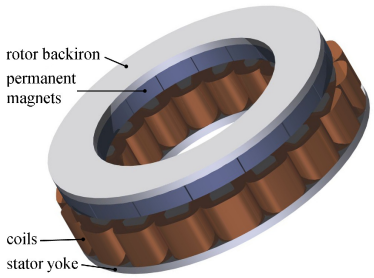

Fig. 1. BLDC drive for a VAD.

II. DRIVE DESIGN

The drive design applied for the efficiency prediction in this paper is depicted in Fig. 1. It consists of a single sided BLDC axial flux drive, developed for operating a LVAD, which provides a perfusion of $6l$ blood per minute against a systemic pressure of $100mmHg$. The ring shaped rotor is made of ferromagnetic steel 9S20, which has a saturation flux density B_{sat} of about $1.7T$. It houses 16 axially alternating magnetized, neodymium iron boron magnets (NdFeB) with a remanent induction B_r of $1.4T$ at $20°C$. The 18 coils, made of a rectangular shaped copper wire are connected into three phase star system that is attached to the ferromagnetic stator yoke (9S20). The copper fill factor amounts to approx. 60%. In the desired operation point the air gap is $1mm$. Table I collects the design parameters of the introduced drive, which are its output torque $T$of $12mNm$, a speed n of $2500rpm$ and its maximum outer dimensions including the air gap between stator and rotor. Due to the single sided drive construction the bearing has to compensate axial attracting forces between stator and rotor [6].

TABLE I
DRIVE PARAMERTERS

design parameters	
nominal speed	2500 rpm
nominal torque	12 mNm
mechanical power	3.14 W
outside diameter	36 mm
drive height	10 mm

978-1-4577-1787-1/12/$26.00 ©2012 IEEE

III. LOSSES IN ELECTRICAL MACHINES

The losses occuring in electrical machines are distinguished into mechanical, copper and iron losses. Mechanical losses are caused by air, gas or liquid friction and by mechanical load. As it is impossible to measure these losses directly, they are commonly estimated to be two percent of the output power [7]. The copper losses are dependent on the resistance of the coils and their current supply. According to:

$$\vec{T} = \vec{r} \times (I \cdot (\vec{l} \times \vec{B})) \quad , \tag{1}$$

the torque depends on the average rotor radius r, active coil length l, and the flux density B in the air gap, which is mostly dependent on the relative angle between stator teeths and the rotor magnets. These parameter are defined by the drive design. So the coil supply supply I depends on the torque requirement. In conclusion the copper losses are a function of the torque requirement as well as the drive design itself. The frequency dependent iron losses can be classified as hysteresis and eddy current losses [8]. When changing the direction of the magnetization of the core material, energy is consumed for the adjustment of the inner structure of the material called Weiss domain. This process causes heat losses, which are proportional to the area enclosed by the hysteresis curve of the core material. According to:

$$P_{hy} = \sigma_{hy} \cdot k_{hy} \cdot \frac{f}{50Hz} (\frac{B}{T})^2 \quad , \tag{2}$$

the hysteresis losses are linear to the operation frequency f of the drive and the square of the flux density B in the core material. The factors σ_{hy} adjustes the rating frequency and flux density of $50Hz$ and $1T$ respectively, while k_{hy} considers the effect of material handling such as punching or cutting lines. Due to the rotor movement, the stator experiences a time dependent change of the magnetic flux density. For this reason eddy currents are induced into the stator teeths, which themselves generate a magnetic field, opposing the changes of the rotor flux density field. This causes losses, which can be calculated by

$$P_{ed} = \sigma_{ed} \cdot k_{ed} \cdot (\frac{f}{50Hz})^2 (\frac{B}{T})^2 \quad . \tag{3}$$

Except from the power of the frequency term, this equation is formally identically to equation 2. Therefore, it should be mentioned that the k-values in these equations differ from each other. Possible methods for determining these values are described in [8]. One option to reduce current losses in radial flux machines is to manufacture the stator of laminations, which are insulated against each other. This however can not be realized for axial flux machines. Their stator is made of solid material as its geometry is too complex for laminations.

IV. LOSS CALCULATION

The basic equation for determing the efficiency of a drive system is given by its output power P_0 and the occuring losses.

$$\eta = \frac{P_o}{P_o + P_{co} + P_{ed}} \tag{4}$$

As this study focuses on the copper P_{co} and eddy current losses P_{ed}, equation 4 does not consider further loss mechanisms. The Finite Elements Method (FEM) simulations described in the following have been performed with the solver package called iMoose, which has been developed at the Institute of Electrical Machines of the RWTH Aachen University [9].

A. COPPER LOSSES

The calculation of the copper losses requires three steps including two FEM simulations. First, the cogging torque has to be determined, which is dependent on the relative position between the permanent magnets in the rotor and the stator teeths. In the next simulation, the coils are supplied with a constant current linkage θ of $50A$. In order to determine the torque, generated by the current linkage, the cogging torque has to be substracted from the simulated torque. As a six step commutation is applied for the control of the drive, the following equation applies:

$$T \sim \Theta_S \Theta_R sin(\varepsilon) \quad . \tag{5}$$

In this equation the generated torque T is a function of the rotor θ_R and stator θ_S current linkages and the sine of the angle ε. Due to its permanent magnet excitation, θ_R is constant and ε is always $90°$. Therefore, the required stator current linkage for generating the required driving torque of $12mNm$ can be obtained by down- or upscaling the torque generated for a current linkage of $50A$. In the last step, the resulting copper losses are calculated.

$$P_{co} = \frac{2}{3} \cdot n_c \cdot \theta^2 \cdot \rho_{co} \cdot \frac{l}{A \cdot cf} (1 + \alpha_{co}(T - T_{20})) \tag{6}$$

In this equation the factor $\frac{2}{3}$ considers the six step commutation control of the drive, where only two out of three phases are supplied simultanously. The copper fill factor cf is assumed to be 60% and θ represents the current linkage in the coils supplying $\frac{2}{3}$ of the n_c coils of the drive. The resistance of one coil is calculated by its resitivity ρ_{co} at room temperature, its wire length l and its cross sectional area A. In order to obtain the resistance at an assumed stator and rotor backiron temperature T of $45°C$, the last term of equation 6, containing the temperature coefficent α_{co} for copper and the room temperature T_{20}, is required.

B. EDDY CURRENT LOSSES

In the introduced drive design, the stator teeth thickness exceeds the eddy current depth. For this reason the skin effect applies, displacing the eddy current from the core of the stator teeths to their edges. As torque is generated in the air gap between stator and rotor, but the eddy currents occur in the stator teeth edges, a modified simulation model of the drive is required. Therefore the eddy current depth δ_{ed} is calculated by

$$\delta_{ed} = \sqrt{\frac{1}{\pi f \sigma \mu}} \quad . \tag{7}$$

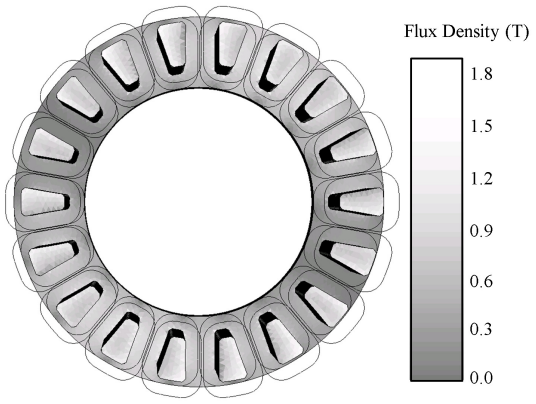

Fig. 2. Saturation of the stator teeth edges.

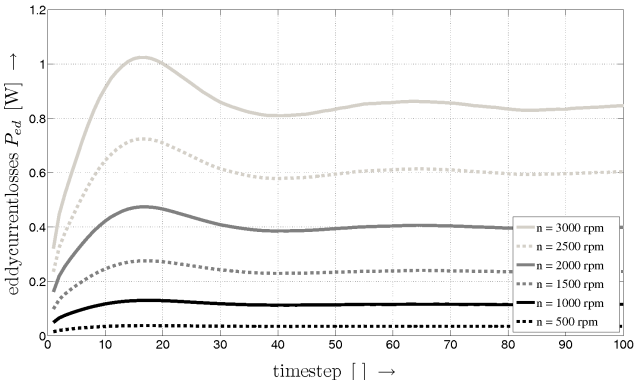

Fig. 3. Eddy current losses for AISI 1006 at various operation speeds.

It depends on the frequency f, the permeability μ of the core material and its conductivity σ. In order to obtain an accurate resolution of the eddy currents at least three element layers per skin depth have to be applied for the FEM simulations. As shown in Fig. 2, the stator teeth edges are partly in saturation due to an increased flux density field at the edges. For this reason, a nonlinear simulation is required.

Additionally, the rotor movement implies for a quasi transient FEM simulation. In transient simulations, establishing a magnet field takes time until a stationary value is reached. According to Fig. 3, the required time steps are rising with the operation frequency of the drive system, but a stationary value is approximattely reached after 80 time steps, what is equivalent to approx. two full rotations of the rotor.

V. SIMULATION RESULTS

Fig. 4 shows the efficiency map for the material AISI 416. It has been obtained by appling equation 4 for various operation points. While the *x*-axis represents the applied torque, the *y*-axis represents the speed and therefore the frequency of the drive. The resulting efficiency can be obtained by comparing the background color of the operation area with the efficiency legend on the right. For the designed nominal operation point at a speed of $2500rpm$ and a torque output of $12mNm$, the efficiency is 77.8% Furthermore this efficiency reveals the general connection between efficiency

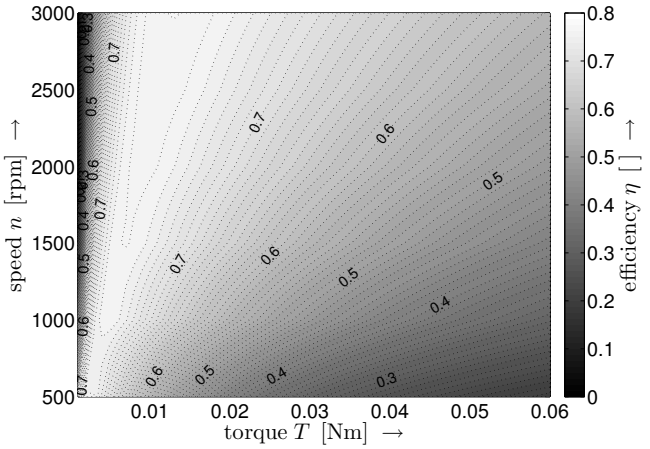

Fig. 4. Efficiency map for AISI 416.

TABLE II
SIMULATION RESULTS

identifier	eddy current losses	efficiency
AISI 416	$335mW$	77.8%
AISI 1006	$601.2mW$	72.8%
AISI 1018	$765.45mW$	70.8%
Vanadium-Permadur	$236.34mW$	79.8%
μ-metal	$493.7mW$	74.7%

and eddy current and copper losses, when following the efficiency deviations along the diagram axes.

The flux density distribution inside the air gap between the stator and the rotor is mostly dependent on the permanent magnet excitation. Due to the relative large virtual air gap, iron saturation has nearly no influence on the torque generation. For this reason, the resulting copper losses amount to $520.8mW$ for all materials. Table II lists the eddy current losses and the resulting efficiency for the studied materials. The lowest eddy current losses ($236.3mW$) and the best efficiency with about 80%, have been determined for Vanadium-Permadur, while the highest eddy current losses ($765.5mW$) and the lowest efficiency have been determined in AISI 1018.

A. MATERIALS

The materials listed in Table III have been studied by applying the described simulation chain. For comparison reasons three types of stainless steel as well as a vanadium-permadur and μ-metal material have been selected. All materials are non grain oriented, have a high saturation flux density and are resistant against corrosion. Therefore, all of them fulfill the operation criteria for the use in VADs. But the materials differ in their conductivity as well as in their magnetic characteristics. For this reason this study provides a generel overview, which materials are suited for the BLDC drive of a VAD system.

B. DISCUSSION

SMC is a powder material consisting of iron particles with an insulating coating. This atomic structure yields a

TABLE III

STUDIED MATERIALS

identifier	material class	conductivity
AISI 416	stainless steel	$1.75 \cdot 10^6 \frac{S}{m}$
AISI 1006	stainless steel	$5.80 \cdot 10^6 \frac{S}{m}$
AISI 1018	stainless steel	$5.80 \cdot 10^6 \frac{S}{m}$
Vanadium-Permadur	cobalt-iron	$2.50 \cdot 10^6 \frac{S}{m}$
μ-metal	nickel alloy	$1.80 \cdot 10^6 \frac{S}{m}$

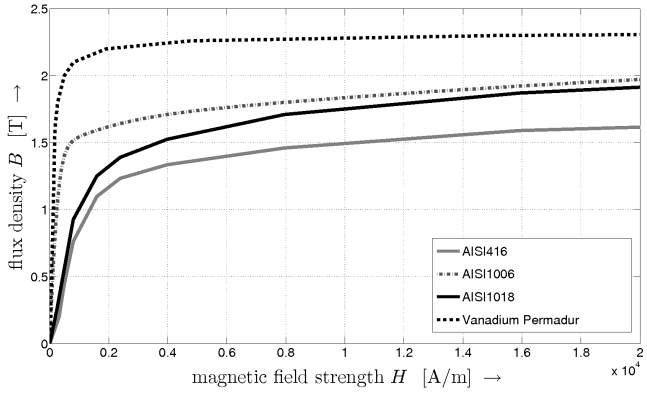

Fig. 5. Flux density vs. magnetic field strength.

minimum of eddy currents. The possibility of casting is beneficial for the production process [10]. But when comparing the relative permeability of SMC $500 < \mu_r \leq 1000$ and iron materials $\mu_r > 5000$, the permeability of SMC is significantly lower. When considering the simulation results, the copper losses are dominating for all studied materials except AISI 1006 and AISI 1018. For this reason SMC materials have been excluded from this study due to their low saturation induction.

At first glance the eddy current losses of AISI 416 are significantly lower than for AISI 1018, because of its significantly lower conductivity. But when comparing AISI 1018 with AISI 1006, the eddy current losses are about 27% lower for AISI 1006, although both materials have the same conductivity. As the B-H curves in Fig. 5 reveal that the flux density is higher for AISI 1006 than for AISI 1018 at the same magnetic field strength, the term k_{ed} in equation 3 is the reason for the higher eddy current losses. This is confirmed by the comparison of AISI 416 and Vanadium Permadur (s. Fig. 6), which is more efficient, although its conductivity and flux density for given magnetic field strengths are higher than for AISI 416. But Vanadium-Permadur is a stiff material, which is difficult and therefore cost intensive to process. When considering that the overall efficiency of the VAD is a product of the efficiencies of the pump and drive system, the 2% less efficient AISI 416 might be the choice for the BLDC drive system due to financial reasons.

VI. CONCLUSIONS

This paper introduced a simplified efficieny prediction chain for a BLDC drive, which has to be extended to consider additional loss mechanisms such as hysterisis losses or eddy

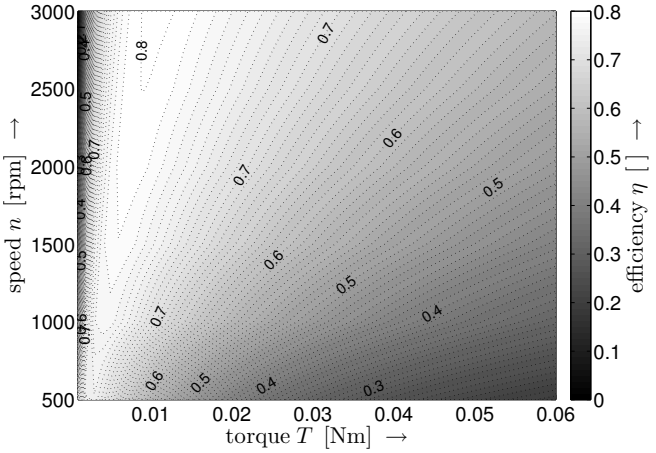

Fig. 6. Efficiency map for Vanadium-Permadur.

current losses in the rotor magnets. Even in its simplified form, it demonstrates that the conductivity or any other single factor is not sufficient for predicting the efficiency of the drive system. Therefore an efficiency prediction muss contain all parameters given in the previous euqations. Further, it must be based on FEM simulations as analytic analysis does not consider nonlinear material characteristics as well as transient behavior. Although the stator yoke of the studied drive design is solid, which supports the propagation of eddy currents, it has been proved that copper losses are dominating for some core materials and up to a frequency of $400Hz$. Therefore SMC materials are no alternative under the given operation conditions due to their low relative permeability, although they surpress eddy currents.

REFERENCES

[1] World-Health-Organization, http://www.who.int/mediacentre/factsheets/, accessed Nov. 2010.

[2] J. G. Copeland, R. Smith, F. Arabia, P. E. Nolan, G. K. Sethi, P. H. Tsau, D. McClellan, and M. J. Slepian, Cardiac replacement with a total artificial heart as a bridge to transplantation, N Engl J Med, vol. 351, pp. 859867, August 2004.

[3] D. Timms, J. Fraser, M. Hayne, J. Dunning, K. McNeil, M. Pearcy, The BiVACOR Rotary Biventricular Assist Device: Concept and In Vitro Investigation, Artificial. Organs, 32(10):816827, Wiley Periodicals, Inc., 2008.

[4] M. Morshuis, M. Schoenbrodt, C. Nojiri, D. Roefe, S. Schulte-Eistrup, J. Boergermann, J. F. Gummert, L. Arusoglu, DuraHeart^{TM} magnetically levitated centrifugal left ventricular assist system for advanced heart failure patients, Expert Rev. Med. Devices 7(2), 173183 (2010).

[5] H. Hoshi, T, Shinshi and S. Takatani, Third-generation blood pumps with mechanical noncontact magnetic bearings, Artificial Organs, 2006, 30(5):324-338, Blackwell Publishing, Inc.

[6] J. F. Gieras, R. J. Wang, M. J. Kamper, Axial Flux Permanent Magnet Brushless Machines, (Book style) 2nd ed. , Springer Verlag, 2008.

[7] D. Hanselmann, Brushless Permanent Magnet Motor Design,2nd ed. , The Writers' Collective, 2006.

[8] G. Bertotti, General Properties of Power Losses in Soft Ferromagnetic Materials, IEEE Transactions on Magnetics , vol.24, no.1, Jan. 1988.

[9] Institute of Electrical Machines, RWTH Aachen University, http://www.iem.rwth-aachen.de, accessed Mar. 2012.

[10] G. Cvetkovski, L. Petkovska, M. Cundev, S. Gair, Improved design of a novel PM disk motor by using soft magnetic composite material, IEEE Transactions on Magnetics , vol.38, no.5, pp. 3165- 3167, Sep 2002